Giant Phonon Anomaly associated with Superconducting Fluctuations in the Pseudogap Phase of Cuprates

Y. H. Liu,[1] R. M. Konik,[2] T. M. Rice,[1,2] and F. C. Zhang[3,4]

[1] *Institut für Theoretische Physik, ETH Zürich, CH-8093, Zürich, Switzerland*
[2] *Condensed Matter Physics and Material Science Department, Brookhaven National Laboratory, Upton, NY 11973*
[3] *Department of Physics, Zhejiang University, Hangzhou, China*
[4] *Collaborative Innovation Center of Advanced Microstructures, Nanjing, China*

arXiv:1506.01258v1 [cond-mat.supr-con] 3 Jun 2015

The opening of the pseudogap in underdoped cuprates breaks up the Fermi surface, which may lead to a breakup of the d-wave order parameter into two subband amplitudes and a low energy Leggett mode due to phase fluctuations between them. This causes a large increase in the temperature range of superconducting fluctuations with an overdamped Leggett mode. Almost resonant scattering of inter-subband phonons to a state with a pair of Leggett modes causes anomalously strong damping. In the ordered state, the Leggett mode develops a finite energy, suppressing the anomalous phonon damping but leading to an anomaly in the phonon dispersion.

The unexpected discovery of a giant anomaly in the dispersion of low energy phonons (GPA) in underdoped pseudogap cuprates has stimulated reconsideration of the role of phonons in cuprate high-T_c superconductors [1–5]. Recently many groups have proposed these anomalies are caused by other electronic instabilities e.g. charge density wave (CDW) order and also pair density wave (PDW) order, which compete with the uniform d-wave pairing state [6–13]. A novel proposal has been put forward by Lee, who argues that Amperean pairing occurs in the pseudogap phase leading to an instability towards PDW and also CDW order [14].

Two recent studies of YBCO samples covering a range of hole densities, found an onset hole density $p_{c1} \sim 0.18$ for the lattice anomalies, which coincides with the onset of the pseudogap [15, 16]. Early photoemission (ARPES) experiments found that the onset of the pseudogap is characterized by a breakup of the Fermi surface into 4 pieces centered on the nodal directions [17]. A rapid expansion of the temperature range of superconducting fluctuations above the transition temperature for long range superconductivity, $T_c(p)$, is also observed [18]. This combination of the onset in hole doping, coinciding with Fermi surface breakup, and the onset in temperature, coinciding with the onset of SC fluctuations, leads us to examine possible consequences of the special disconnected nature of the Fermi surface in the pseudogap phase, on d-wave superconductivity. We find that superconducting fluctuations in an extended temperature above T_c can result as a special feature of d-wave superconductivity in the presence of the pseudogap. We shall show below that these fluctuations in turn can couple to finite wavevector phonons leading to GPA. In our model the lattice fluctuations are dynamic as argued by LeTacon et al [4, 15] but random static CDW can still be induced by local perturbations, such as the random acceptors in nearly all underdoped cuprates [16]. The stoichiometric underdoped cuprate $YBa_2Cu_4O_8$ is an exception. The NMR/NQR experiments by Suter et al [19] found dynamic charge fluctuations but no static lattice ordered modulation in agreement with earlier NMR experiments [20, 21]. A recent detailed NMR study of YBCO found evidence for static lattice distortions, possibly induced around lattice imperfections by GPA. They also did not report systematic splitting of the NMR lines which would be evidence for long range ordered CDW [16].

In our microscopic model the key ingredient is the novel breakup of the full Fermi surface into 4 disconnected pieces that characterizes the pseudogap phase. In the superconducting phase, the 4 pieces combine to give 2 sets of Cooper pairs with nodes along $(1, 1)$ and $(1, \bar{1})$. This breakup opens the possibility of superconducting phase fluctuations not just of the overall Josephson phase, but between the disconnected sets of Cooper pairs. The possibility of phase fluctuations between separated pieces of the Fermi surface in multiband s-wave superconductors, i.e. the Leggett mode (LM), was studied by Leggett [22] many years ago. The superconductivity in cuprates has d-wave symmetry with nodes on the pockets and the accompanying sign changes reduce the net coupling between the two sets. We propose this can lead to a low energy LM.

Representation of Fermi surface

One-loop Renormalization Group calculations of the single band Hubbard model near ½-filling, show that at low energies the Coulomb repulsion develops substantial structure in **k**-space, peaking at momentum transfers (π, π) in both the particle-hole spin triplet and particle-particle singlet channels [23, 24]. The latter drives d-wave pairing with maximum amplitudes at antinodal. Yang et al [25, 26] argued the transition into the pseudogap phase is driven by increasing Umklapp scattering, which

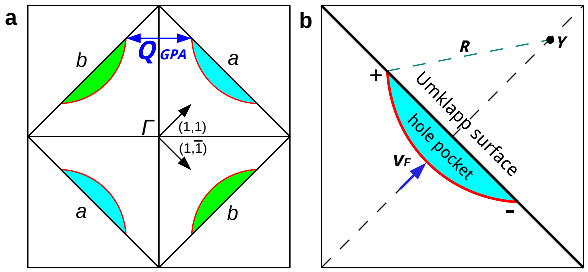

Figure 1: **Representation of the band structure by Fermi arcs. a,** The breakup of Fermi surface to 2 subbands a & b in $(1,1)$ & $(1,\bar{1})$ directions. $\mathbf{Q}_{\mathrm{GPA}}$ is a wavevector connecting the two subbands, which is also the wavevector of phonon anomaly. **b,** Simplified model of Fermi arcs. Each Fermi arc is represented by a circular arc (shown red) with center $\mathbf{Y}$, radius R, and terminates at the Umklapp surface. The Fermi velocity $\mathbf{v}_F$ (blue arrow) is assumed to have constant magnitude on the whole arc. $\mathbf{Y}$ is uniquely determined by the choices of the wavevector between arc tips to be 0.51π, and the hole concentration $p = 11.5\%$. These are typical values in ARPES experiment. $\pm$ denotes the sign of symmetry factor $\gamma_{\mathbf{p}}$.

converts the antinodal gaps to insulating. They put forward an ansatz based on a modified BCS self energy with an energy gap pinned to the Umklapp surface leading to anisotropic Fermi pockets centered on the nodal directions. Later detailed ARPES experiments confirmed anisotropic nodal Fermi pockets [27]. The superconducting complex pairing amplitude is confined to 2 disconnected pairs of pockets centered on the $(1,1)$ & $(1,\bar{1})$ directions, illustrated in Fig. 1. We shall refer to these as subband a & b respectively. An examination of the pair scattering processes shows that there are intra-subband (π,π) processes. But the inter-subband processes connecting subbands a & b involve cancellations between pairing and depairing scattering processes with similar wavevectors in a d-wave state. For this reason when we write the pairing scattering in terms of intra-subband and inter-subband processes for a d-wave state, we propose that the intra-subband pairing is stronger than the inter-subband pairing, similar to the pairing model examined by Leggett [22].

For simplicity the anisotropic nodal Fermi pockets will be represented as Fermi arcs (see Fig. 1) with a constant Fermi velocity along the arc. The parameters are chosen from a recent paper by Comin et al [28].

Leggett Mode and Fluctuations

Assuming that both intra-subband and inter-subband couplings U and J are separable d-wave forms with symmetry factor, $\gamma_{\mathbf{p}}$, allows us to obtain the fluctuation pair propagator from the following Bethe-Salpeter equation

$$L_q = \begin{pmatrix} U & J \\ J & U \end{pmatrix} - \begin{pmatrix} U & J \\ J & U \end{pmatrix} \begin{pmatrix} \pi_q^{(a)} & 0 \\ 0 & \pi_q^{(b)} \end{pmatrix} L_q \qquad (1)$$

for L_q, in terms of which the full anisotropic fluctuation is written as $L_{pp'q} = \gamma_{\mathbf{p}} L_q \gamma_{\mathbf{p}'}$ with $q = (\mathbf{q}, iq_0)$. The electronic bubble $\pi_q^{(i)} = \frac{1}{\beta V}\sum^{(i)}_{\mathbf{p},i\omega} \gamma^2_{\mathbf{p}} G_{\frac{\mathbf{q}}{2}+\mathbf{p},iq_0+i\omega} G_{\frac{\mathbf{q}}{2}-\mathbf{p},-i\omega}$ is defined on both sets of Fermi arcs for $i = a, b$. We denote zero-temperature, finite-temperature, and retarded Green's functions by $G_{\mathbf{p},\omega}$, $G_{\mathbf{p},i\omega}$, and $G^R_{\mathbf{p},\omega}$ respectively, similarly for other quantities. In the temperature region $T_c < T < T_o$ (onset of superconducting fluctuations), the electron's retarded Green's function takes the form $G^R_{\mathbf{p},\omega} = \left[\omega - \epsilon_{\mathbf{p}} + i\Gamma^{(e)}\right]^{-1}$, where $\epsilon_{\mathbf{p}}$ is the Fermi arc dispersion and $\Gamma^{(e)} = aT + bT^2$ is a temperature dependent quasiparticle damping [29]. The retarded propagator for the fluctuating LM is derived to be

$$L^R_{\mathbf{q},\omega} = \frac{T}{cN_0}\frac{1}{i\omega - \Gamma^{(\mathrm{LM})}_{\mathbf{q}}}\left(\frac{1}{2} - \frac{1}{2}\sigma_x\right). \qquad (2)$$

See the supplementary information (SI) for details. This form of the fluctuation propagator describes an overdamped bosonic mode. Here N_0 is the density of states per spin at the Fermi energy for one pair of arcs, the constant $c = \frac{1}{4\pi}\psi'\left[\frac{1}{2} + \frac{1}{2\pi}(a + bT_c)\right]$ with $\psi(x)$ the digamma function. The damping of the LM $\Gamma^{(\mathrm{LM})}_{\mathbf{q}} = \tau^{-1} + Dq^2$, in which the inverse relaxation time $\tau^{-1} = \frac{T}{c}\log\frac{T}{T_c} + 2bT(T - T_c) + \frac{T}{cN_0}2|J|/\left(U^2 - J^2\right)$ and the diffusion constant $D = -\frac{v_F^2}{16\pi T}\psi''\left[\frac{1}{2} + \frac{1}{2\pi}(a + bT)\right]/\psi'\left[\frac{1}{2} + \frac{1}{2\pi}(a + bT_c)\right]$ are functions of the temperature. The uniform damping rate τ^{-1} decreases as long range order at T_c is approached.

We take zero temperature as a representative case for the ordered phase. In this case the LM is derived similarly to equation (1), but with a different form of the electronic bubble [22, 30, 31] $\pi_q^{(i)} = \frac{1}{V}\sum^{(i)}_{\mathbf{p}}\int\frac{d\omega}{2\pi i}\gamma^2_{\mathbf{p}}\left(G_{\frac{\mathbf{q}}{2}+\mathbf{p},\frac{q_0}{2}+\omega} G_{\frac{\mathbf{q}}{2}-\mathbf{p},\frac{q_0}{2}-\omega} + F_{\frac{\mathbf{q}}{2}+\mathbf{p},\frac{q_0}{2}+\omega} F_{\frac{\mathbf{q}}{2}-\mathbf{p},\frac{q_0}{2}-\omega}\right)$. $G_{\mathbf{p},\omega} = (\omega + \epsilon_{\mathbf{p}})/Z$ and $F_{\mathbf{p},\omega} = \Delta_{\mathbf{p}}/Z$ are the normal and anomalous Green's functions, where $Z = \omega^2 - E^2_{\mathbf{p}} + i\delta$ and $\delta \to 0^+$. $E_{\mathbf{p}} = \sqrt{\epsilon^2_{\mathbf{p}} + \Delta^2_{\mathbf{p}}}$ is the quasiparticle energy and $\Delta_{\mathbf{p}} = \gamma_{\mathbf{p}}\Delta$ is the d-wave gap function. It follows (see SI)

$$L_{\mathbf{q},\omega} = \frac{4\Delta^2}{N_0}\frac{1}{\omega^2 - \omega^2_{\mathbf{q}} + i\delta}\left(\frac{1}{2} - \frac{1}{2}\sigma_x\right) \qquad (3)$$

with a LM dispersion $\omega^2_{\mathbf{q}} = \omega_0^2 + \frac{1}{2}v_F^2 q^2$. In this case, the LM is a coherent bosonic mode with infinite lifetime. The LM is gapped, and its frequency at zero momentum satisfies $\omega_0^2 = \frac{4\Delta^2}{N_0}2|J|/\left(U^2 - J^2\right)$. Usually the ratio $\frac{\omega_0}{2\Delta} < 1$.

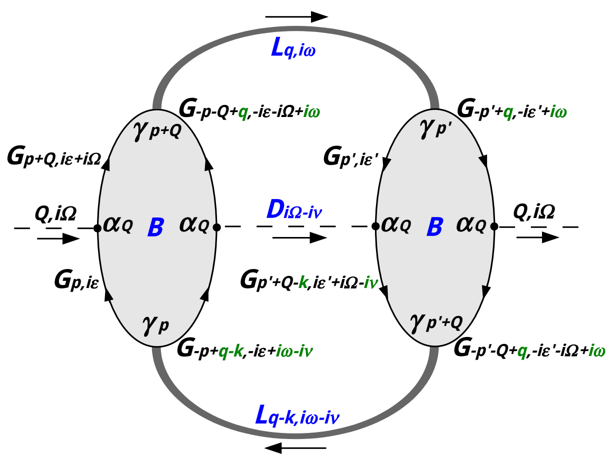

Figure 2: **Feynman diagram of phonon self energy due to the interaction with Leggett mode.** B is the effective interaction vertex consisting of a particle-particle electronic bubble (G is the electron Green's function). The intermediate state consists of two Leggett modes (L) and one phonon (D). Due to the separation of energy scales between Leggett mode and the electron, all quantities in green are neglected.

Phonon Self Energy

The $\mathbf{k}$-space separation of the two bands does not move the LM away from $\mathbf{q} = 0$, since this phase mode involves the transfer of zero momentum Cooper pairs between the subbands. Nonetheless it involves moving charges between the subbands. Absorption and emission of phonons with the appropriate wavevectors also causes a charge transfer, but now as single quasiparticles, between the two subbands. Therefore it is not unexpected that a coupling between these processes should exist. In particular, we find the coupling is largest in the temperature region $T \sim T_c$, where the LM drops to zero energy and becomes overdamped. To this end we consider the process outlined in Fig. 2, where an incoming phonon is scattered to a nearby phonon wavevector with emission and absorption of LM fluctuations. Such a process does not occur in standard superconductors but can exist here because of a soft overdamped LM for $T_c < T < T_o$. Below we summarize calculations of the phonon self energy in two temperature regions.

First we look at the phonon damping in the range of strong SC fluctuations starting at the onset temperature T_o of the SC fluctuations down to the superconducting transition temperature T_c. The expression for the phonon self energy Π, corresponding to the Feynman diagram Fig. 2, follows

$$
\begin{aligned}
\Pi_{\mathbf{Q},i\Omega} &= 4\alpha_{\mathbf{Q}}^4 B_{\mathbf{Q},i\Omega}^2 I_{i\Omega}, \quad I_{i\Omega} = \frac{1}{V^2}\sum_{\mathbf{q},\mathbf{k}} \mathrm{Tr} I_{\mathbf{q},\mathbf{k},i\Omega}, \\
I_{\mathbf{q},\mathbf{k},i\Omega} &= \frac{1}{\beta^2}\sum_{i\omega,i\nu} L_{\mathbf{q},i\omega} L_{\mathbf{q}-\mathbf{k},i\omega-i\nu} D_{i\Omega-i\nu}, \\
B_{\mathbf{Q},i\Omega} &= \frac{1}{\beta V}\sum_{\mathbf{p},i\epsilon} \gamma_{\mathbf{p}}\gamma_{\mathbf{p}+\mathbf{Q}} \\
&\quad \times G_{\mathbf{p},i\epsilon} G_{-\mathbf{p},-i\epsilon} G_{\mathbf{p}+\mathbf{Q},i\epsilon+i\Omega} G_{-\mathbf{p}-\mathbf{Q},-i\epsilon-i\Omega},
\end{aligned}
\tag{4}
$$

where $\alpha_{\mathbf{Q}}$ is the electron-phonon coupling constant, $I_{\mathbf{q},\mathbf{k},i\Omega}$ is the frequency summation over the intermediate state consisting of two LMs and one phonon, $B_{\mathbf{Q},i\Omega}$ is the effective interaction vertex between phonons and LMs, and $D_{i\Omega} = 2\Omega_0/\left[(i\Omega)^2 - \Omega_0^2\right]$ is the bare Green's function for phonons with an assumed flat dispersion $\Omega_{\mathbf{Q}} = \Omega_0$. We have chosen the simplest form of the effective interaction, B and ignore damping due to quasiparticle excitations, keeping only $\mathrm{Re}B^R_{\mathbf{Q},\Omega}$, to concentrate on the novel phonon damping caused by the presence of a soft LM. Note, $\mathrm{Re}B^R_{\mathbf{Q},\Omega_0}$ has a strong dependence on the phonon wavevector $\mathbf{Q}$ (see Fig. 3) and peaks at a wavevector joining the ends of the arcs, because the symmetry factors and the available phase space for the transition at this wavevector are both large. We checked that $\mathrm{Im}B^R_{\mathbf{Q},\Omega_0} \ll \mathrm{Re}B^R_{\mathbf{Q},\Omega_0}$ for this set of parameters. $\mathrm{Re}B^R_{\mathbf{Q},\Omega_0}$ also shows a peak at $\mathbf{Q} = 0$ which will be discussed later.

The effective interaction vertex B involves an integration over the whole Brillouin zone and all frequencies, while the LM L is only well-defined for small momenta and frequencies. This leads to a separation of spatial and temporal scales and enables us to ignore all small wavevectors and frequencies (marked green in Fig. 2) in calculating B. Aided by the similarity with the Aslamazov-Larkin diagram [32–36], we perform analytical calculation for I^R_Ω. For $|\Omega - \Omega_0| \ll \Omega_0$, it follows (see SI for details)

$$
\begin{aligned}
I^R_\Omega &= \frac{2\pi}{D^2}\frac{T^4}{c^2 N_0^2}\int_0^\infty dx\, p(x)\, \frac{1}{\Omega - \Omega_0 + \frac{2i(1+x)}{\tau}}, \\
p(x) &= \int_0^{2\pi} d\theta \frac{\arctan\left[\sqrt{\frac{\cos^2\theta}{(1+x)^2 - x^2\cos^2\theta}}\, x\right]}{\sqrt{\cos^2\theta\left[(1+x)^2 - x^2\cos^2\theta\right]}}.
\end{aligned}
\tag{5}
$$

In this region the on-shell values satisfy $\mathrm{Re}I^R_{\Omega_0} = 0$ and $\mathrm{Im}I^R_{\Omega_0} < 0$. The temperature dependence of the imaginary part of the retarded phonon self energy $\mathrm{Im}\Pi^R$ i.e. the phonon damping, is plotted in Fig. 3. The self energy has a peak in momentum space at $\mathbf{Q} = (Q_{\mathrm{GPA}}, 0)$, near to the tip to tip wavevector between two sets of Fermi arcs. Because of the factor τ in equation (5), the temperature dependence shows anomalous behavior at the long range critical temperature T_c, in agreement with experiment [4].

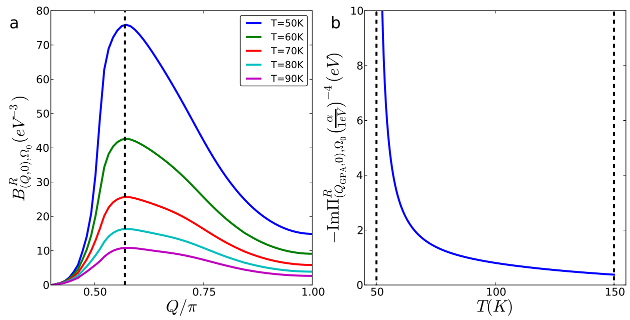

Figure 3: **GPA in the fluctuation region. a,** Temperature and momentum dependence of the effective interaction vertex B, with the dashed line marking Q_{GPA}. **b,** The anomalous phonon damping. Parameters: Fermi velocity $v_F = 500\mathrm{meV}$, bare phonon frequency $\Omega_0 = 10\mathrm{meV}$, ratio between Leggett mode frequency at $\mathbf{q} = 0$ and the superconducting gap $\frac{\omega_0}{2\Delta} = 0.1$, quasiparticle damping $\Gamma^{(e)} = 0.5T + \left(0.3\mathrm{meV}^{-1}\right) T^2$, and the long range order temperature $T_c = 50\mathrm{K}$. We used an energy cutoff of $\pm100\mathrm{meV}$ around the Fermi surface, which does not affect the qualitative feature of GPA.

Below T_c, there is a finite restoring force for inter-subband phase fluctuations and the LM develops a finite energy at $\mathbf{q} = 0$, which raises the energy of the intermediate state in Fig. 2. As a consequence the approximate resonant condition between the incoming phonon and the intermediate state with a scattered phonon and 2 LMs no longer holds, leading to a suppression of the phonon damping at low T. The GPA changes its form at $T < T_c$ with strongly reduced damping. An anomaly in the phonon dispersion appears due to virtual coupling to an excited intermediate state. Treating the low temperature behavior at $T = 0$, the factor from the intermediate state becomes

$$\begin{aligned} \mathrm{Tr} I_{\mathbf{q},\mathbf{k},\Omega} &= \mathrm{Tr} \int \frac{d\omega}{2\pi i}\frac{d\nu}{2\pi i} L_{\mathbf{q},\omega} L_{\mathbf{q}-\mathbf{k},\omega-\nu} D_{\Omega-\nu} \\ &= \frac{4\Delta^4}{N_0^2}\frac{1}{\omega_{\mathbf{q}}\omega_{\mathbf{q}-\mathbf{k}}}\frac{2\left(\Omega_0+\omega_{\mathbf{q}}+\omega_{\mathbf{q}-\mathbf{k}}\right)}{\Omega^2-\left(\Omega_0+\omega_{\mathbf{q}}+\omega_{\mathbf{q}-\mathbf{k}}\right)^2+i\delta} \end{aligned} \tag{6}$$

where $D_\Omega = 2\Omega_0/\left(\Omega^2 - \Omega_0^2 + i\delta\right)$. We conclude that in this region, the on-shell values satisfy $\mathrm{Re} I^R_{\Omega_0} < 0$ and $\mathrm{Im} I^R_{\Omega_0} = 0$, in agreement with the experiment for $T < T_c$ [4].

At long wavelengths, $\mathbf{Q} \sim 0$, the long range nature of the Coulomb interaction suppresses the response in metals at low frequencies to any perturbation coupling to the total electronic density. The electron-phonon interaction introduced in equation (4) couples equally to both subbands and as a result the associated scattering processes are suppressed at $\mathbf{Q} \sim 0$.

Summary and Conclusions

As we remarked earlier the transition into the pseudogap phase at the hole density $p_{c1} \sim 0.18$ displays three strong anomalies simultaneously — an antinodal insulating energy gap leading to a breakup of the Fermi surface into 4 nodal pockets, a rapid expansion of the temperature range of superconducting fluctuations, and the appearance of a giant phonon anomaly in this temperature range. These phenomena are unique to the underdoped cuprates. Our aim here is to put forward a microscopic scenario which explains the interrelation between these phenomena. The low energy Coulomb interaction must be strong to drive the partial truncation of the Fermi surface, which is a precursor to a full Mott gap at zero doping [25, 26]. A weakness of our microscopic scenario is the need to assume a form for this effective Coulomb interaction. Our choice is guided by the evolution found by Functional Renormalization Group in the overdoped density region [23, 24]. The persistence of d-wave symmetry even as the maximally gapped antinodal regions transform from a superconducting to an insulating gap, leads to the conditions for a low energy LM to emerge. As we discuss above, this novel assumption enables us to consistently explain all three anomalies. In particular we can explain the temperature evolution of the GPA from increasing damping as $T \to T_c$ from above, to a GPA with vanishing damping but a dispersion anomaly at $T < T_c$. Here we considered only zero magnetic field. The recent analyses of quantum oscillation experiments at high magnetic fields are consistently explained by a coherent orbit around all four arcs, is intriguing [37]. It raises the question of the evolution of the LM with increasing magnetic field for future study.

[1] Chang, J. *et al.* Direct observation of competition between superconductivity and charge density wave order in $YBa_2Cu_3O_{6.67}$. *Nature Physics* **8**, 871–876 (2012).

[2] Ghiringhelli, G. *et al.* Long-range incommensurate charge fluctuations in $(Y,Nd)Ba_2Cu_3O_{6+x}$. *Science* **337**, 821–825 (2012).

[3] Achkar, A. J. *et al.* Distinct charge orders in the planes and chains of ortho-III-ordered $YBa_2Cu_3O_{6+\delta}$ superconductors identified by resonant elastic X-ray scattering. *Phys. Rev. Lett.* **109**, 167001 (2012).

[4] Le Tacon, M. *et al.* Inelastic X-ray scattering in $YBa_2Cu_3O_{6.6}$ reveals giant phonon anomalies and elastic central peak due to charge-density-wave formation. *Nature Physics* **10**, 52–58 (2014).

[5] Blackburn, E. *et al.* X-ray diffraction observations of a charge-density-wave order in superconducting ortho-II $YBa_2Cu_3O_{6.54}$ single crystals in zero magnetic field. *Phys. Rev. Lett.* **110**, 137004 (2013).

[6] Hayward, L. E., Hawthorn, D. G., Melko, R. G. & Sachdev, S. Angular fluctuations of a multicomponent

order describe the pseudogap of $YBa_2Cu_3O_{6+x}$. *Science* **343**, 1336–1339 (2014).
[7] Efetov, K. B., Meier, H. & Pepin, C. Pseudogap state near a quantum critical point. *Nature Physics* **9**, 442–446 (2013).
[8] Bulut, S., Atkinson, W. A. & Kampf, A. P. Spatially modulated electronic nematicity in the three-band model of cuprate superconductors. *Phys. Rev. B* **88**, 155132 (2013).
[9] Melikyan, A. & Norman, M. R. Symmetry of the charge density wave in cuprates. *Phys. Rev. B* **89**, 024507 (2014).
[10] Fradkin, E., Kivelson, S. A. & Tranquada, J. M. Theory of intertwined orders in high temperature superconductors. *arXiv:1407.4480* (2014).
[11] Tsvelik, A. M. & Chubukov, A. V. Composite charge order in the pseudogap region of the cuprates. *Phys. Rev. B* **89**, 184515 (2014).
[12] Chowdhury, D. & Sachdev, S. The enigma of the pseudogap phase of the cuprate superconductors. *arXiv:1501.00002* (2015).
[13] Wang, Y., Agterberg, D. F. & Chubukov, A. Coexistence of charge-density-wave and pair-density-wave orders in underdoped cuprates. *arXiv:1501.07287* (2015).
[14] Lee, P. A. Amperean pairing and the pseudogap phase of cuprate superconductors. *Phys. Rev. X* **4**, 031017 (2014).
[15] Blanco-Canosa, S. *et al.* Resonant x-ray scattering study of charge-density wave correlations in $YBa_2Cu_3O_{6+x}$. *Phys. Rev. B* **90**, 054513 (2014).
[16] Wu, T. *et al.* Incipient charge order observed by NMR in the normal state of $YBa_2Cu_3O_y$. *Nature Commun.* **6**, 6438 (2015).
[17] Norman, M. R. *et al.* Destruction of the Fermi surface in underdoped high-T_c superconductors. *Nature* **392**, 157–160 (1998).
[18] Dubroka, A. *et al.* Evidence of a precursor superconducting phase at temperatures as high as 180K in $R\mathrm{Ba_2Cu_3O_{7-\delta}}(R = \mathrm{Y, Gd, Eu})$ superconducting crystals from infrared spectroscopy. *Phys. Rev. Lett.* **106**, 047006 (2011).
[19] Suter, A., Mali, M., Roos, J. & Brinkmann, D. Charge degree of freedom and the single-spin fluid model in $YBa_2Cu_4O_8$. *Phys. Rev. Lett.* **84**, 4938–4941 (2000).
[20] Machi, T. *et al.* Nuclear spin-lattice relaxation and Knight shift in $YBa_2Cu_4O_8$. *Physica C: Superconductivity* **173**, 32–36 (1991).
[21] Mangelschots, I. *et al.* ^{17}O NMR study in aligned $YBa_2Cu_4O_8$ powder. *Physica C: Superconductivity* **194**, 277–286 (1992).
[22] Leggett, A. J. Number-phase fluctuations in two-band superconductors. *Progress of Theoretical Physics* **36**, 901–930 (1966).
[23] Honerkamp, C., Salmhofer, M., Furukawa, N. & Rice, T. M. Breakdown of the Landau-Fermi liquid in two dimensions due to Umklapp scattering. *Phys. Rev. B* **63**, 035109 (2001).
[24] Honerkamp, C., Salmhofer, M. & Rice, T. M. Flow to strong coupling in the two-dimensional Hubbard model. *Eur. Phys. J. B* **27**, 127–134 (2002).
[25] Yang, K.-Y., Rice, T. M. & Zhang, F.-C. Phenomenological theory of the pseudogap state. *Phys. Rev. B* **73**, 174501 (2006).
[26] Rice, T. M., Yang, K.-Y. & Zhang, F. C. A phenomenological theory of the anomalous pseudogap phase in underdoped cuprates. *Reports on Progress in Physics* **75**, 016502 (2012).
[27] Yang, H.-B. *et al.* Reconstructed Fermi surface of underdoped $Bi_2Sr_2CaCu_2O_{8+\delta}$ cuprate superconductors. *Phys. Rev. Lett.* **107**, 047003 (2011).
[28] Comin, R. *et al.* Charge order driven by Fermi-arc instability in $Bi_2Sr_{2-x}La_xCuO_{6+\delta}$. *Science* **343**, 390–392 (2014).
[29] Buhmann, J. M., Ossadnik, M., Rice, T. M. & Sigrist, M. Numerical study of charge transport of overdoped $La_{2-x}Sr_xCuO_4$ within semiclassical Boltzmann transport theory. *Phys. Rev. B* **87**, 035129 (2013).
[30] Leggett, A. J. Theory of a superfluid Fermi liquid. I. general formalism and static properties. *Phys. Rev.* **140**, A1869–A1888 (1965).
[31] Leggett, A. J. Theory of a superfluid Fermi liquid. II. collective oscillations. *Phys. Rev.* **147**, 119–130 (1966).
[32] Aslamasov, L. & Larkin, A. The influence of fluctuation pairing of electrons on the conductivity of normal metal. *Physics Letters A* **26**, 238–239 (1968).
[33] Schmidt, H. The onset of superconductivity in the time dependent Ginzburg-Landau theory. *Zeitschrift für Physik* **216**, 336–345 (1968).
[34] Yip, S.-K. Fluctuations in an impure unconventional superconductor. *Phys. Rev. B* **41**, 2612–2615 (1990).
[35] Koshelev, A. E., Varlamov, A. A. & Vinokur, V. M. Theory of fluctuations in a two-band superconductor: MgB_2. *Phys. Rev. B* **72**, 064523 (2005).
[36] Larkin, A. & Varlamov, A. *Theory of Fluctuations in Superconductors* (Oxford Science Publications, 2005).
[37] Sebastian, S. E. *et al.* Normal-state nodal electronic structure in underdoped high-T_c copper oxides. *Nature* **511**, 61–64 (2014).

Acknowledgements

The authors acknowledge M. Sigrist, A. M. Tsvelik, J. Chang, W. Q. Chen, J. Gukelberger, D. Manske, M. Troyer, L. Wang, S. Z. Zhang, and Y. Zhou for helpful discussions. Y.H.L. is supported by ERC grant No. 290464. R.M.K. is supported by the US DOE under contract number DE-AC02-98 CH 10886. F.C.Z. is partly supported by NSFC grant 11274269 and National Basic Research Program of China (No. 2014CB921203).

Author contributions

The calculations were performed by Y.H.L. with assistance from T.M.R. All authors discussed the results and took part in the preparation of the manuscript.

Additional information

Supplementary information is available in the online version of the paper. Reprints and permissions information is available online at www.nature.com/reprints.

Correspondence and requests for materials should be addressed to T.M.R.

Competing financial interests

The authors declare no competing financial interests.